A Appendix

A.1 NAS Search Spaces

NASBench-101[1] introduces a large and expressive search space with 423k unique convolutional neural architectures and training statistics on CIFAR-10. NASBench-201[2] contains the training statistics of 15,625 architectures across three different datasets, including CIFAR-10, CIFAR-100, and Tiny-ImageNet-16. Network Design Spaces (NDS) dataset[3] [1] with PYCLS [2] codebase [4] provides trained neural networks from 11 search spaces including DARTS [3], AmoebaNet [4], ENAS [5], NASNet [6], PNAS [7], ResNet [8], ResNeXt [9], etc. A search space with "-f" suffix stands for a search space that has fixed number of layers and channels. The ResNeXt-A and ResNeXt-B have different channel-number and group-convolution settings. NASBench-NLP[5] [10] is an NLP neural architecture search space, including 14k recurrent cells trained on the Penn Treebank (PTB) [11] dataset.

A.2 Experiment Setup

For **CNN** architecture training, the learning rate is $1\mathrm{e}{-1}$ and the weight decay is $1\mathrm{e}{-5}$. Each architecture is trained for 100 iterations on a single batch of data using SGD optimizer [12]. All the convolutional architectures use the same setting. The size of the input images is $h = w = 32$ and the size of output feature maps is $h' = w' = 8$. For **RNN** training, the learning rate is $1\mathrm{e}{-3}$, the weight decay is $1.2\mathrm{e}{-6}$, the batch size b is 16, and the sequence length l is 8. Each architecture is trained for 100 iterations on a single batch of data using the Adam optimizer [13].

A.2.1 Regularized Evolutionary Algorithm

Algorithm 1 Regularized Evolutionary Algorithm in General

Initialize an empty population queue, Q_pop `// The maximum population is` P
Initialize an empty set, $history$ `// Will contain all visited individuals`
for $i = 1, 2, \cdots, P$ **do**
    $new\_individual \leftarrow$ RandomInit()
    $new\_individual.fitness \leftarrow$ Eval($new\_individual$)
    Enqueue(Q_pop, $new\_individual$)`// Add individual to the right of` Q_pop
    Add $new\_individual$ to $history$
end
`// Evolve for` T_iter
for $i = 1, 2, \cdots, T\_iter$ **do**
    Initialize an empty set, $sample\_set$
    for $i = 1, 2, \cdots, S$ **do**
        Add an individual to $sample\_set$ from Q_pop without replacement.
        `// The individual stays in` Q_pop
    end
    $parent \leftarrow$ the individual with best fitness in $sample\_set$
    $child \leftarrow$ Mutate($parent$)
    $child.fitness \leftarrow$ Eval($child$)
    Enqueue(Q_pop, $child$)
    Add $child$ to $history$
    Dequeue(Q_pop)`// Remove the oldest individual from the left of` Q_pop
end
return the individual with best fitness in $history$

Regularized Evolutionary Algorithm [4] (RE) combines the tournament selection [14] with the aging mechanism which remove the oldest individuals from the population each round. We show a general form of RE in Alg. 1. Aging evolution aims to explore the search space more extensively, instead of

[1] `https://github.com/google-research/nasbench`
[2] `https://github.com/D-X-Y/NAS-Bench-201`
[3] `https://github.com/facebookresearch/nds`
[4] `https://github.com/facebookresearch/pycls`
[5] `https://github.com/fmsnew/nas-bench-nlp-release`

focusing on the good models too early. Works [15, 16, 17] also suggest that the RE is suitable for neural architecture search. Since we aim to develop a general NAS evaluator (as the fitness function in RE), we conduct fair comparisons between GenNAS and other methods without fine-tuning or any tricks (e.g., warming-up). Hence, we constantly use the setting $P = 50$, $S = 10$, $T\_iter = 400$ for all the search experiments.

A.2.2 Proxy Task Search

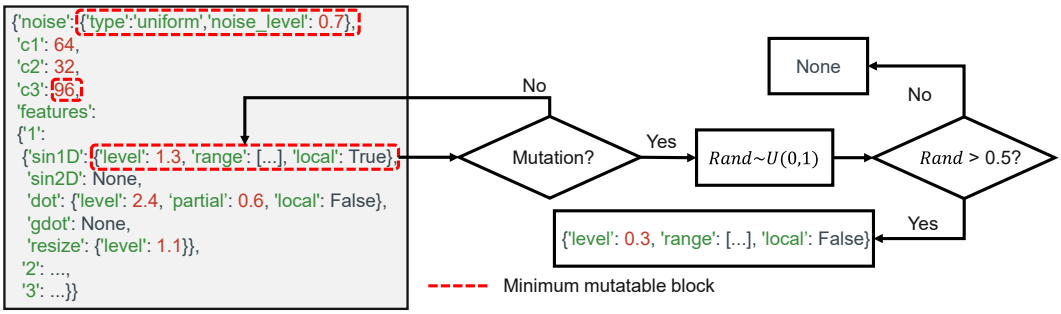

Figure 1: The configuration of a task in JSON style and the illustration of task mutation.

The configuration of a task is shown in Fig. 1. We introduce the detailed settings of different signal bases. (1) `Noise` is chosen from standard `Gaussian` distribution ($\mathcal{N}(0,1)$) or `uniform` distribution ($\mathcal{U}(-1,1)$). The generated noise maps are directly multiplied by the `level` which can be selected from 0 to 1 with a step of 0.1. (2) `Sin1D` generates 2D synthetic feature maps using different frequencies choosing from the `range`, which contains 10 frequencies sampled from $[a, b]$, where a and b are sampled from 0 to 0.5 with the constraint $0 < a < b < 0.5$. (3) `Sin2D` uses the similar setting as `Sin1D`, where both the f_x and f_y for a 2D feature map are sampled from the `range`. (4) C_i can be selected from $\{16, 32, 48, 64, 96\}$. Other settings are already described in Section 3.1.2. During the mutation, each minimum mutatable block (including signal definitions and the number of channels) has 0.2 probability to be regenerated as shown in Fig. 1. For RNN settings, we search for both the input and output synthetic signal tensors. The dimension d is chosen from $\{16, 32, 48, 64, 96\}$.

A.2.3 End-to-end NAS

In the end-to-end NAS, GenNAS is incorporated in the RE as the fitness function to explore the search space. For **NASBench-101**, the mutation rate for each vertice is $1/|v|$ where $|v| = 7$. More details of the search space NASBench-101 can be found in the original paper [16]. For **NASBench-201**, the mutation rate for each edge is $1/|e|$ where $|e| = 6$. More details of the search space NASBench-101 can be found in the original paper [15]. For **NDS** ResNet series, the sub search space consists of 25000 sampled architectures from the whole search space. We apply mutation in RE by randomly sampling 200 architectures from the sub search space and choosing the most similar architecture as the child. For **NASBench-NLP**, we follow the work [10] by using the graph2vec [18] features find the most similar architecture as the child.

A.3 Additional Experiments

A.3.1 Regression vs. Classification Using Same Training Samples

We study effectiveness of regression using 10 tasks searched on NASBench-101, varying the batch size from 1 to 1024. The ranking correlation achieved by GenNAS using regression is plotted in Fig. 2a. We also plot the classification task performances with single-batch data in Fig. 2b. Apparently, using the same amount of data, the ranking correlation achieved by classification (ρ around 0.85) is much worse than regression (ρ around 0.3).

A.3.2 Batch Sizes and Iterations

We show the effect of batch size by using 10 tasks searched on NASBench-101. We use batch sizes varied from 1 to 1024 and plot the ranking results in Fig. 2a. We find that 16 as the batch

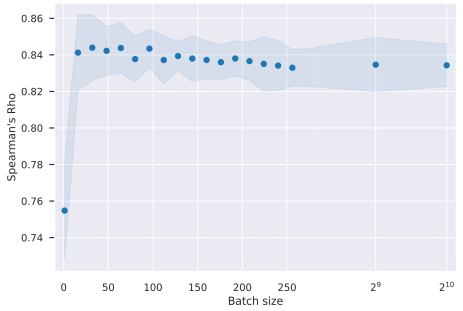

(a) Regression (GenNAS) ranking correlation averaged from 10 searched tasks using different batch sizes.

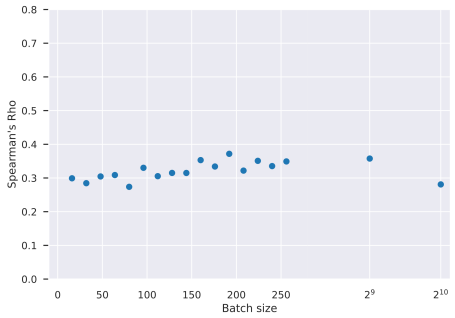

(b) Classification task's ranking correlation using the same setting as (a).

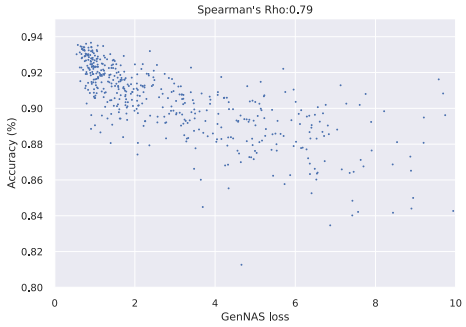

(c) Classification accuracy vs. GenNS regression loss with batch size 1.

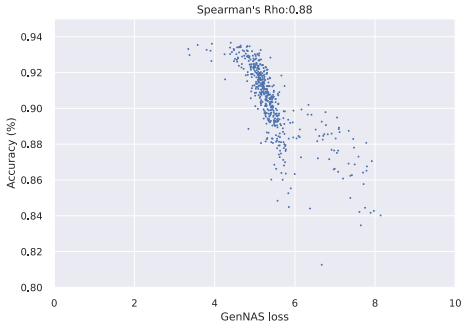

(d) Classification accuracy vs. GenNS regression loss with batch size 16.

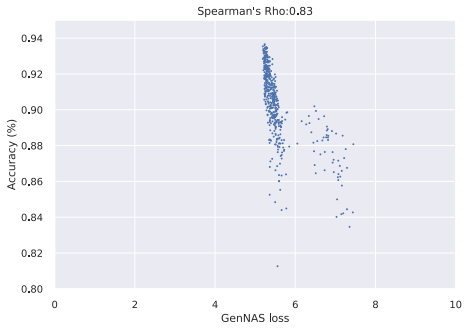

(e) Classification accuracy vs. GenNS regression loss with batch size 1024.

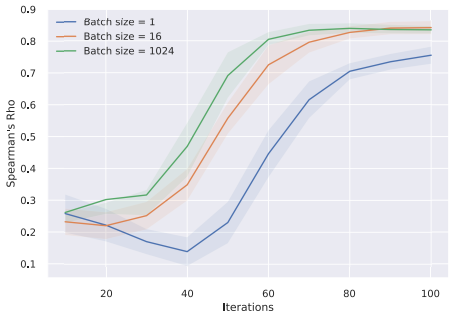

(f) 10 searched tasks' ranking correlation on NASBench-101 using different numbers of iterations.

Figure 2: (a) Regression (GenNAS) ranking correlation averaged from 10 searched tasks on NASBench-101 in terms of Spearman's ρ with batch size in $\{1, 16, 32, ..., 256, 512, 1024\}$. (b) Classification task's ranking correlation using the same amount of data in (a). (c) Classification accuracy using a searched task on NASBench-101 with batch size as 1 on CIFAR-10. The y-axis is the groundtruth (CIFAR-10 accuracy) and the x-axis is the GenNAS regression loss. (d) Similar to (c), batch size as 16. (e) Similar to (c), batch size as 1024. (f) 10 searched tasks ranking performance (in terms of Spearman's ρ) on NASBench-101 using different iterations.

size is adequate for a good ranking performance. Also, we observe a small degradation when batch size increases and then becomes stable as the batch size keeps increasing. Hence, We plot the ranked architecture distribution with a searched task using 1, 16, 1024 as batch size respectively on Fig. 2c, 2d, 2e. We observe that when only using a single image, the poor-performance architectures can also achieve similar regression losses as the good architectures. It suggests that the task is too easy to distinguish the differences among architectures. Also, 1024 as batch size leads to the higher regression losses of best architectures. It suggests that a very challenging task is also hard for good

architectures to learn and may lead to slight ranking performance degradation. In addition, we plot the ranking performance using different numbers of iterations in Fig. 2f. It shows that 100 iterations is necessary for the convergence of ranking performance.

A.3.3 Sensitivity Studies of Random Seeds and Initialization

Table 1: Ranking correlation (Spearman's ρ) analysis of different 10 seeds across three different search spaces with the searched tasks on them respectively. For the NASBench-101, the 500 architecture samples [19] are constantly used for evaluation. For DARTS and ResNet search spaces, 1000 samples are randomly sampled with different seeds from the evaluated architecture sets provided by NDS [1].

Search Space	0	1	2	3	4	5	6	7	8	9	Average
NASBench-101	0.880	0.850	0.875	0.869	0.872	0.874	0.877	0.863	0.872	0.872	0.870±0.008
DARTS	0.809	0.899	0.861	0.831	0.841	0.836	0.851	0.841	0.885	0.861	0.850±0.025
ResNet	0.860	0.853	0.841	0.810	0.865	0.877	0.874	0.804	0.808	0.803	0.840±0.029

Random Seeds. We rerun the 3 searched tasks on their target search spaces (NASBench-101, DARTS, ResNet) for 10 runs with different random seeds. The results are shown in Table 1. GenNAS demonstrates its robustness across different random seeds.

Table 2: Ranking correlation (Spearman's ρ) analysis of 10 searched tasks on NASBench-101 with different initialization methods.

Weight init	Bias init	0	1	2	3	4	5	6	7	8	9	Average
Default	Default	0.835	0.860	0.860	0.878	0.835	0.810	0.859	0.832	0.816	0.828	0.841±0.021
Kaiming	Default	0.844	0.854	0.857	0.856	0.832	0.818	0.854	0.746	0.829	0.811	0.830±0.032
Xavier	Default	0.856	0.881	0.863	0.874	0.849	0.825	0.865	0.830	0.838	0.851	0.853±0.018
Default	Zero	0.867	0.882	0.854	0.880	0.848	0.847	0.874	0.808	0.848	0.850	0.856±0.021
Kaiming	Zero	0.845	0.842	0.856	0.861	0.828	0.821	0.846	0.770	0.823	0.823	0.831±0.025
Xavier	Zero	0.859	0.876	0.869	0.879	0.839	0.842	0.861	0.828	0.846	0.843	0.854±0.016

Initialization. We perform an experiment to evaluate the effects of different initialization for 10 searched tasks on NASBench-101. For the weights, we use the default PyTorch initialization, Kaiming initialization [20], and Xavier initialization [21]. For the bias, we use the default PyTorch initialization and zeroized initialization. The results are shown in Table 2. We observe that for some specific tasks (e.g., task 7), Kaiming initialization may lead to lower ranking correlation. Also, zeroized bias initialization slightly increases the ranking correlation. However, overall, GenNAS shows stable performance across different initialization methods.

A.3.4 Kendall Tau and Retrieving Rates

For the sample experiments on NASBench-101/201/NLP and NDS, we report the performance of our methods compared to other efficient NAS approaches' in Table 3 by Kendall τ [22]. We define the retrieving rate@topK as $\frac{\#\{\text{Pred@TopK}\cap\text{GT@TopK}\}}{\#\{\text{GT@TopK}\}}$, where $\#$ is the operator of cardinality, GT@TopK and Pred@TopK are the set of architectures that are ranked in the top-K of groundtruths and predictions respectively. We report the retrieving rate@Top10% for all the search spaces in Table 4. Moreover, we report the retrieving rate@Top5%-Top50% for GenNAS-COMBO and GenNAS-N on NASBench-101 with other 1000 random sampled architectures in Table 5.

A.3.5 End-to-end NAS Architectures

Here we visualize all the ImageNet DARTS cell architectures: searched by GenNAS-combo, searched by GenNAS-D14 in Fig 3 and Fig 4 respectively.

A.3.6 GPU Performance

We use the PyTorch 1.5.0 [26], on a desktop with I7-6700K CPU, 16 GB RAM and a GTX 1080 Ti GPU (11GB GDDR5X memory) to evaluate the GPU performance of GenNAS. The results are shown in Table 6.

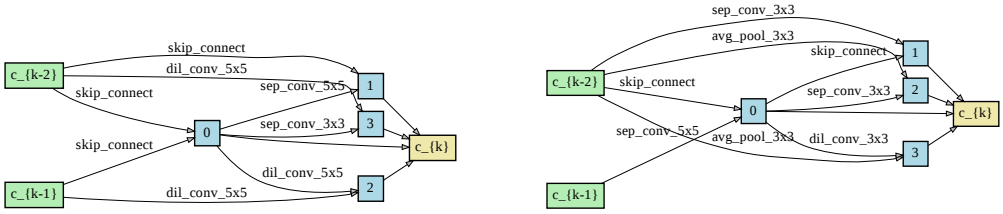

(a) Normal cell (b) Reduce cell

Figure 3: Cell architectures (normal and reduce) searched by GenNAS-combo

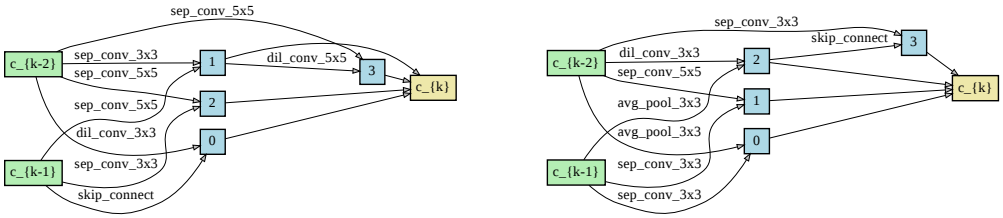

(a) Normal cell (b) Reduce cell

Figure 4: Cell architectures (normal and reduce) searched by GenNAS-D14

Table 3: GenNAS' ranking correlation evaluation comparing with other efficient NAS approaches using the Kendall τ.

NASBench-101					
Dataset	NASWOT [23]	synflow [24]	**GenNAS**		
			single	combo	search-N
CIFAR-10	0.27	0.24	0.59	0.66	**0.7**
ImgNet	0.36	0.14	0.47	**0.54**	0.53

NASBench-201								
Dataset	NASWOT	synflow	jacob_cov	snip	EcoNAS [25]	**GenNAS**		
						single	combo	search-N
CIFAR-10	0.6	0.52	0.59	0.41	0.62	0.57	0.67	**0.71**
CIFAR-100	0.63	0.57	0.53	0.46	0.57	0.52	0.63	**0.65**
ImgNet16	0.6	0.54	0.56	0.44	0.57	0.53	0.61	**0.67**

Neural Design Spaces								
Dataset	NAS-Space	NASWOT	synflow	**GenNAS**				
				single	combo	search-N	search-D	search-R
CIFAR-10	DARTS	0.48	0.3	0.3	0.45	0.52	**0.68**	0.63
	DARTS-f	0.21	0.09	0.36	**0.43**	0.37	0.42	0.36
	Amoeba	0.21	0.06	0.36	0.47	0.5	**0.59**	0.53
	ENAS	0.39	0.13	0.39	0.49	0.48	**0.63**	0.59
	ENAS-f	0.31	0.2	0.46	**0.55**	0.49	0.53	0.48
	NASNet	0.3	0.02	0.4	0.5	0.47	**0.58**	0.52
	PNAS	0.36	0.17	0.22	0.37	0.42	**0.57**	0.52
	PNAS-f	0.09	0.18	0.31	0.38	0.39	**0.38**	0.33
	ResNet	0.19	0.14	0.23	0.38	0.38	0.38	**0.64**
	ResNeXt-A	0.46	0.32	0.4	0.5	0.6	0.45	**0.65**
	ResNeXt-B	0.4	0.43	0.17	0.3	0.37	0.38	**0.52**
ImageNet	DARTS	0.49	0.14	0.43	0.52	0.52	**0.66**	0.48
	DARTS-f	0.13	0.25	0.49	**0.57**	0.48	0.51	0.42
	Amoeba	0.33	0.17	0.46	0.53	0.55	**0.62**	0.5
	ENAS	0.51	0.12	0.4	0.47	0.4	**0.63**	0.48
	NASNet	0.39	0.01	0.36	0.42	0.37	**0.5**	0.43
	PNAS	0.45	0.11	0.19	0.27	0.31	**0.45**	0.3
	ResNeXt-A	0.52	0.28	0.61	**0.7**	0.56	0.44	0.69
	ResNeXt-B	0.45	0.21	0.53	0.65	0.39	0.43	**0.67**

NASBench-NLP			
Dataset	**GenNAS**		
	single	combo	search
PTB	0.43	0.55	0.63

Table 4: GenNAS' retrieving rate@top10% comparing with other efficient NAS approaches. For the NASBench-101 we use the set of 500 architectures that sampled by Liu, et al. [19] for obtaining the ImageNet groundtruth.

NASBench-101

Dataset	number of samples	NASWOT [23]	synflow [24]	GenNAS single	GenNAS combo	GenNAS search-N
CIFAR-10	500	32%	28%	58%	64%	**68%**
ImgNet	500	36%	14%	52%	54%	**64%**

NASBench-201

Dataset	number of samples	NASWOT	synflow	jacob_cov	snip	EcoNAS [25]	GenNAS single	GenNAS combo	GenNAS search-N
CIFAR-10	1000	43%	48%	27%	27%	52%	43%	36%	**53%**
CIFAR-100	1000	48%	47%	23%	36%	47%	46%	46%	**58%**
ImgNet16	1000	49%	43%	33%	32%	41%	48%	40%	**51%**

Neural Design Spaces

Dataset	number of samples	NAS-Space	NASWOT	synflow	GenNAS single	GenNAS combo	GenNAS search-N	GenNAS search-D	GenNAS search-R
CIFAR-10	1000	DARTS	29%	10%	16%	43%	45%	**59%**	49%
	1000	DARTS-f	1%	5%	22%	**33%**	18%	22%	23%
	1000	Amoeba	20%	4%	20%	39%	45%	**50%**	40%
	1000	ENAS	31%	6%	25%	48%	41%	**57%**	48%
	1000	ENAS-f	28%	2%	34%	**45%**	42%	38%	37%
	1000	NASNet	33%	7%	27%	38%	**46%**	52%	43%
	1000	PNAS	24%	9%	21%	39%	**46%**	44%	37%
	1000	PNAS-f	6%	4%	21%	27%	**31%**	25%	22%
	1000	ResNet	7%	4%	38%	44%	38%	54%	**64%**
	1000	ResNeXt-A	28%	25%	25%	**61%**	53%	52%	58%
	1000	ResNeXt-B	21%	30%	10%	13%	36%	40%	**71%**
ImageNet	121	DARTS	17%	0%	50%	58%	55%	**58%**	18%
	499	DARTS-f	8%	4%	33%	27%	35%	**39%**	24%
	124	Amoeba	33%	0%	50%	42%	58%	**58%**	41%
	117	ENAS	36%	9%	18%	18%	45%	**55%**	45%
	122	NASNet	33%	0%	42%	**50%**	42%	33%	33%
	119	PNAS	10%	9%	45%	36%	45%	**55%**	9%
	130	ResNeXt-A	31%	8%	67%	67%	50%	33%	**75%**
	164	ResNeXt-B	38%	13%	38%	50%	33%	38%	**64%**

NASBench-NLP

Dataset	number of samples	grad	norm	snip	grasp	fisher	synflow	GenNAS single	GenNAS combo	GenNAS search
PTB	1000	10%	10%	4%	-	22%	38%	38%	47%	**63%**

Table 5: Retrieving rate@top5%-top50% of GenNAS-combo/N on 1000 randomly sampled architectures on NASBench-101.

Method	@top5%	@top10%	@top20%	@top30%	@top40%	@top50%
GenNAS-combo	0.6	0.6	0.73	0.74	0.79	0.82
GenNAS-N	0.56	0.58	0.66	0.76	0.80	0.85

Table 6: Evaluations of GenNAS' GPU performance. We test GenNAS with 6 different batch sizes from 16 to 96. "A/B" denotes: A (second) as the average one-iteration run time for the search space, and B (GB or gigabyte) as the GPU memory usage. "OOM" means some large models may lead to the out-of-memory issue for the target GPU.

Search Space	B-size 16	B-size 32	B-size 48	B-size 64	B-size 80	B-size 96
NASBench-101	0.023/0.78	0.023/0.92	0.023/1.12	0.022/1.22	0.023/1.41	0.023/1.56
NASBench-201	0.020/0.77	0.020/0.93	0.021/1.12	0.020/1.24	0.020/1.46	0.020/1.62
DARTS	0.049/1.92	0.056/3.39	0.069/5.07	0.088/6.88	0.103/7.62	OOM
DARTS-f	0.077/1.42	0.088/2.21	0.104/3.30	0.122/3.79	0.145/5.15	0.171/6.07
Amoeba	0.080/2.53	0.103/4.38	0.128/6.60	0.159/9.25	0.194/6.85	OOM
ENAS	0.059/2.40	0.076/4.31	0.090/5.84	0.115/7.78	0.140/9.15	OOM
ENAS-f	0.095/1.67	0.111/2.58	0.134/3.70	0.159/4.54	0.186/6.31	0.216/7.53
NASNet	0.061/2.23	0.073/3.77	0.094/5.83	0.116/6.87	0.140/8.68	0.160/9.30
PNAS	0.074/2.52	0.097/4.36	0.121/6.53	0.155/8.23	0.189/9.42	OOM
PNAS-f	0.114/1.69	0.143/2.67	0.173/4.03	0.208/4.83	0.250/6.24	0.293/7.45
ResNet	0.016/1.28	0.016/1.54	0.016/2.05	0.016/2.34	0.016/2.34	0.016/2.77
ResNeXt-A	0.025/1.65	0.025/2.82	0.026/4.55	0.027/6.86	0.028/9.75	0.029/5.92
ResNeXt-B	0.022/1.98	0.022/3.47	0.023/5.63	0.024/7.33	0.027/9.51	0.029/5.95
NASBench-NLP	0.029/0.90	0.029/0.90	0.029/0.90	0.029/0.90	0.029/0.93	0.029/0.94

References

[1] Ilija Radosavovic, Justin Johnson, Saining Xie, Wan-Yen Lo, and Piotr Dollár. On network design spaces for visual recognition. In *Proceedings of the IEEE/CVF International Conference on Computer Vision*, pages 1882–1890, 2019.

[2] Ilija Radosavovic, Raj Prateek Kosaraju, Ross Girshick, Kaiming He, and Piotr Dollár. Designing network design spaces. In *CVPR*, 2020.

[3] Hanxiao Liu, Karen Simonyan, and Yiming Yang. Darts: Differentiable architecture search. *arXiv preprint arXiv:1806.09055*, 2018.

[4] Esteban Real, Alok Aggarwal, Yanping Huang, and Quoc V Le. Regularized evolution for image classifier architecture search. In *Proceedings of the aaai conference on artificial intelligence*, volume 33, pages 4780–4789, 2019.

[5] Hieu Pham, Melody Guan, Barret Zoph, Quoc Le, and Jeff Dean. Efficient neural architecture search via parameters sharing. In *International Conference on Machine Learning*, pages 4095–4104. PMLR, 2018.

[6] Barret Zoph, Vijay Vasudevan, Jonathon Shlens, and Quoc V Le. Learning transferable architectures for scalable image recognition. In *Proceedings of the IEEE conference on computer vision and pattern recognition*, pages 8697–8710, 2018.

[7] Chenxi Liu, Barret Zoph, Maxim Neumann, Jonathon Shlens, Wei Hua, Li-Jia Li, Li Fei-Fei, Alan Yuille, Jonathan Huang, and Kevin Murphy. Progressive neural architecture search. In *Proceedings of the European conference on computer vision (ECCV)*, pages 19–34, 2018.

[8] Kaiming He, Xiangyu Zhang, Shaoqing Ren, and Jian Sun. Deep residual learning for image recognition. In *Proceedings of the IEEE conference on computer vision and pattern recognition*, pages 770–778, 2016.

[9] Saining Xie, Ross Girshick, Piotr Dollár, Zhuowen Tu, and Kaiming He. Aggregated residual transformations for deep neural networks. In *Proceedings of the IEEE conference on computer vision and pattern recognition*, pages 1492–1500, 2017.

[10] Nikita Klyuchnikov, Ilya Trofimov, Ekaterina Artemova, Mikhail Salnikov, Maxim Fedorov, and Evgeny Burnaev. Nas-bench-nlp: neural architecture search benchmark for natural language processing. *arXiv preprint arXiv:2006.07116*, 2020.

[11] Mitchell Marcus, Beatrice Santorini, and Mary Ann Marcinkiewicz. Building a large annotated corpus of english: The penn treebank. 1993.

[12] Ilya Sutskever, James Martens, George Dahl, and Geoffrey Hinton. On the importance of initialization and momentum in deep learning. In *International conference on machine learning*, pages 1139–1147. PMLR, 2013.

[13] Diederik P Kingma and Jimmy Ba. Adam: A method for stochastic optimization. *arXiv preprint arXiv:1412.6980*, 2014.

[14] David E Goldberg and Kalyanmoy Deb. A comparative analysis of selection schemes used in genetic algorithms. In *Foundations of genetic algorithms*, volume 1, pages 69–93. Elsevier, 1991.

[15] Xuanyi Dong and Yi Yang. Nas-bench-201: Extending the scope of reproducible neural architecture search. *arXiv preprint arXiv:2001.00326*, 2020.

[16] Chris Ying, Aaron Klein, Eric Christiansen, Esteban Real, Kevin Murphy, and Frank Hutter. Nas-bench-101: Towards reproducible neural architecture search. In *International Conference on Machine Learning*, pages 7105–7114. PMLR, 2019.

[17] Yukang Chen, Gaofeng Meng, Qian Zhang, Shiming Xiang, Chang Huang, Lisen Mu, and Xinggang Wang. Renas: Reinforced evolutionary neural architecture search. In *Proceedings of the IEEE/CVF Conference on Computer Vision and Pattern Recognition*, pages 4787–4796, 2019.

[18] Annamalai Narayanan, Mahinthan Chandramohan, Rajasekar Venkatesan, Lihui Chen, Yang Liu, and Shantanu Jaiswal. graph2vec: Learning distributed representations of graphs. *arXiv preprint arXiv:1707.05005*, 2017.

[19] Chenxi Liu, Piotr Dollár, Kaiming He, Ross Girshick, Alan Yuille, and Saining Xie. Are labels necessary for neural architecture search? In *European Conference on Computer Vision*, pages 798–813. Springer, 2020.

[20] Kaiming He, Xiangyu Zhang, Shaoqing Ren, and Jian Sun. Delving deep into rectifiers: Surpassing human-level performance on imagenet classification. In *Proceedings of the IEEE international conference on computer vision*, pages 1026–1034, 2015.

[21] Xavier Glorot and Yoshua Bengio. Understanding the difficulty of training deep feedforward neural networks. In *Proceedings of the thirteenth international conference on artificial intelligence and statistics*, pages 249–256. JMLR Workshop and Conference Proceedings, 2010.

[22] Maurice G Kendall. A new measure of rank correlation. *Biometrika*, 30(1/2):81–93, 1938.

[23] Joseph Mellor, Jack Turner, Amos Storkey, and Elliot J Crowley. Neural architecture search without training. *arXiv preprint arXiv:2006.04647*, 2020.

[24] Mohamed S Abdelfattah, Abhinav Mehrotra, Łukasz Dudziak, and Nicholas D Lane. Zero-cost proxies for lightweight nas. *arXiv preprint arXiv:2101.08134*, 2021.

[25] Dongzhan Zhou, Xinchi Zhou, Wenwei Zhang, Chen Change Loy, Shuai Yi, Xuesen Zhang, and Wanli Ouyang. Econas: Finding proxies for economical neural architecture search. In *Proceedings of the IEEE/CVF Conference on Computer Vision and Pattern Recognition*, pages 11396–11404, 2020.

[26] Adam Paszke, Sam Gross, Francisco Massa, Adam Lerer, James Bradbury, Gregory Chanan, Trevor Killeen, Zeming Lin, Natalia Gimelshein, Luca Antiga, Alban Desmaison, Andreas Kopf, Edward Yang, Zachary DeVito, Martin Raison, Alykhan Tejani, Sasank Chilamkurthy, Benoit Steiner, Lu Fang, Junjie Bai, and Soumith Chintala. Pytorch: An imperative style, high-performance deep learning library. In H. Wallach, H. Larochelle, A. Beygelzimer, F. d'Alché-Buc, E. Fox, and R. Garnett, editors, *Advances in Neural Information Processing Systems 32*, pages 8024–8035. Curran Associates, Inc., 2019.